DAMAGE PROGRESSION ANALYSIS IN 3-D WOVEN COMPOSITE COMPONENTS

F. Coman[1] , S. John[1], and I. Herszberg[2]

1. Royal Melbourne Institute of Technology, University, Department of Mechanical & Manufacturing Engineering,
Bundoora East Campus, Vic. 3083, Australia.
2. Royal Melbourne Institute of Technology, University, Department of Aerospace Engineering, The Sir Lawrence Wackett Centre for Aerospace Design Technology,
GPO Box 2476V, Melbourne, 3001, Australia.

SUMMARY: This work addresses the issue of micro-structural damage of the woven during a deformation process, primarily in the tensile mode. This paper investigates damage initiation and progression in three dimensional multilayer woven glass reinforced plastics (GRP) subjected to uniaxial tensile and shear loading. Two composites made of multilayer woven architectures, hereby named: Orthogonal and Normal Layer Interlock form the basis of this study; It identifies the physical characteristics which initiate the various damage modes, what these modes are and when they occur. During tensile tests, specimens were photographed at various load levels using transmitted light to monitor internal damage. These photographs assisted in the identification of the various stages of failure, and when they occurred. In all cases cracks occurred in the tows both normal and parallel to the testing direction.

KEYWORDS: Woven Architectures, Disbonding, Internal Damage, Reduced stiffness, Transverse Cracks, Uniaxial tensile Loading,

INTRODUCTION

The notion of inherent process-induced damage in woven composite structures has been lucidly reported in the literature [1], [2], [3], [4], [5], [9]. In some of these reports, attempts at quantifying and identifying these damage mechanisms have been made with various degrees of success. Also, in recent papers such as [6] and [9], evidence of geometry-induced damage during the loading process is reported.

Two composites made of multilayer woven architectures, hereby named: Orthogonal and Normal Layer Interlock form the basis of this study; see Figures 1a and 1b. The woven E-glass preforms were consolidated with a vinyl ester resin using resin transfer moulding. Tensile specimens were cut in the warp and weft directions and tested to failure.

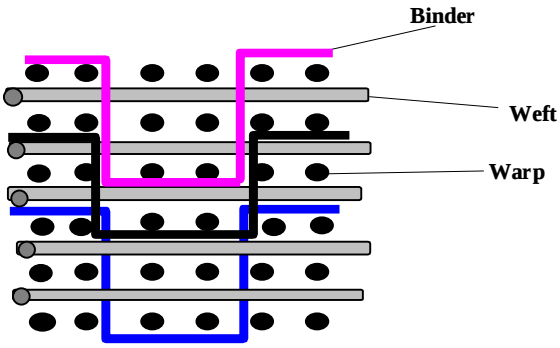

Figure 1a Orthogonal through-thickness binder

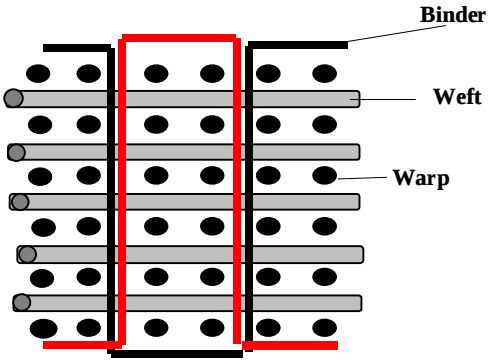

Figure 1b Normal Layer interlock

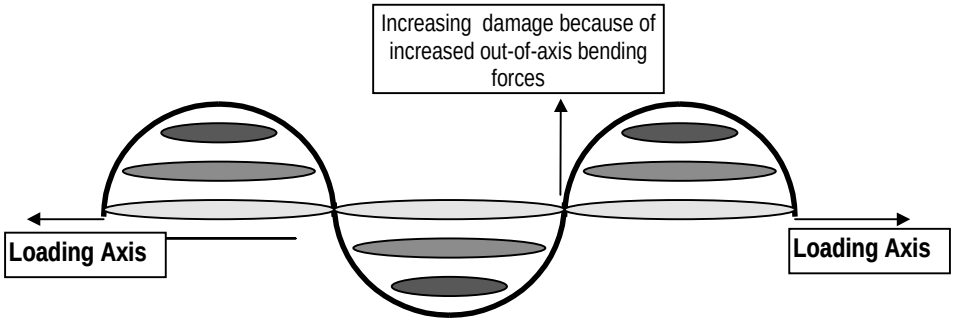

Figure 2 Schematic of suspected mechanics responsible for binder-inflicted damage

Two composites made of multilayer woven architecture, Orthogonal and Normal Layer Interlock formed the basis of this study. The woven E-glass preforms were consolidated with vinyl ester resin using Resin Transfer Moulding process [1].

Tensile specimens were cut in the warp and weft directions and tested to failure. Material elastic properties were calculated in order to differentiate those structures. During tensile tests, specimens were photographed at various load levels using transmitted light to monitor internal damage. These photographs assisted in the identification of the various stages of failure, and when they occurred. In all cases cracks occurred in the tows in both the normal and parallel directions to the testing. Furthermore, when tested in the warp direction, the Normal Layer Interlock specimen developed local disbonding between the warp tow and matrix below the binder. Figure 2 illustrates how this might mechanistically occur.

The two types of architectures had slightly differing failure characteristics, in both size and shape, occurring at different load levels. The transverse cracks reduced the

stiffness of the specimens by lowering the contribution of perpendicular tows to composite stiffness. The longitudinal cracks and local disbonds had a small effect on stiffness [1].

Three areas are identified as being the cause of this reduction in strength: crimping of fibres, resin rich areas and damage to the fibres during the weaving process. Different types of architecture have been designed to reduce fibre crimping and disperse resin rich areas in an attempt to improve the mechanical properties of the material.

Tensile damage progression.

The form of the stress-strain plot and the features observed in transmitted light photographs were similar for all types of architecture tested in both directions. Observation during testing and microscopic examination (post-test) revealed several damage features in the specimens and these are summarized in Table 1 and Figure 3 below.

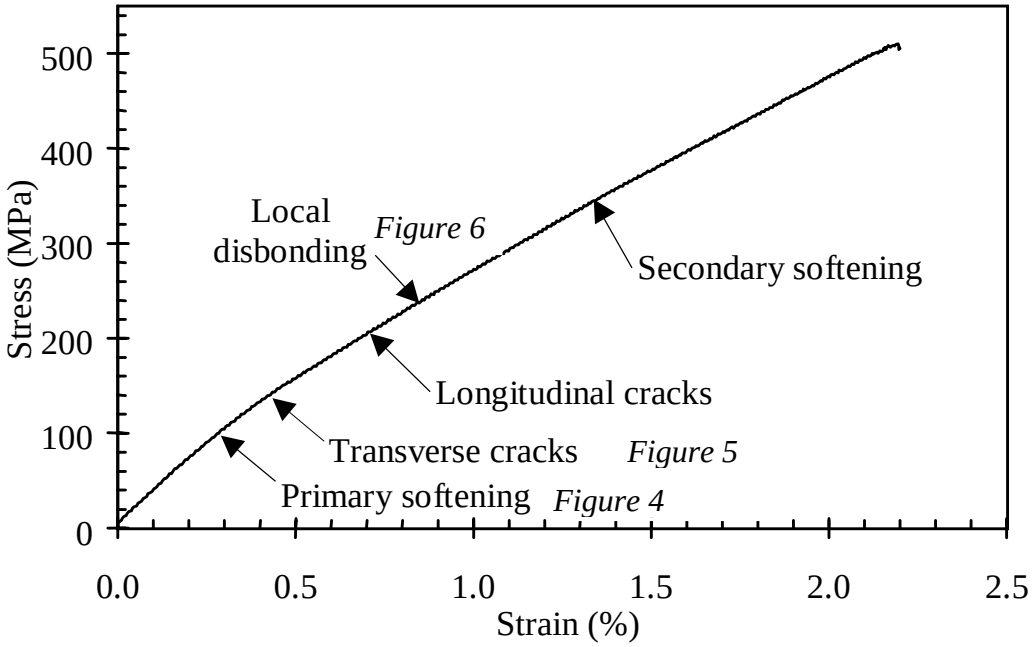

Figure 3 Summary of Loading History in direct Tension

Figure 4 Transmitted light photograph showing a sample at the primary softening point

Damage features	Orthogonal Testing direction		Normal layered Testing direction	
	Warp	**Weft**	**Warp**	**Weft**
Primary softening (με)	3240	3571	3588	2756
Modulus drop (%)	26	25	29	19
Appearance of transverse cracks (με)	6810	5250	3800	5940
Appearance of longitudinal cracks (με)	None*	None	8220	14900
Appearance of local disbonding (με)	None*	None	13200	None
Secondary softening (με)	14324	13584	15902	13060
Modulus drop (%)	8	5	13	5

* Data unavailable

Table 1. Average strain at which stiffness changes and damage features were observed

Primary softening. A 20 to 30 % reduction in stiffness was observed for all the specimen at about 3000 με. It was explained by the appearance of the transverse cracks which are cracks within the perpendicular to the loading direction tow. This is shown in Figure 4.

Transverse cracks. Some specimens developed straight transverse cracks, whilst other transverse cracks followed a more or less sinusoidal path, that will be explained later. They were initiated on between 3040 and 7160 με and occurred in all the specimens. Figure 5 shows that these cracks appeared exclusively in the tow transverse to the testing direction. The crack numbers increased with the load until about 50% of failure load, when the saturation occurred.

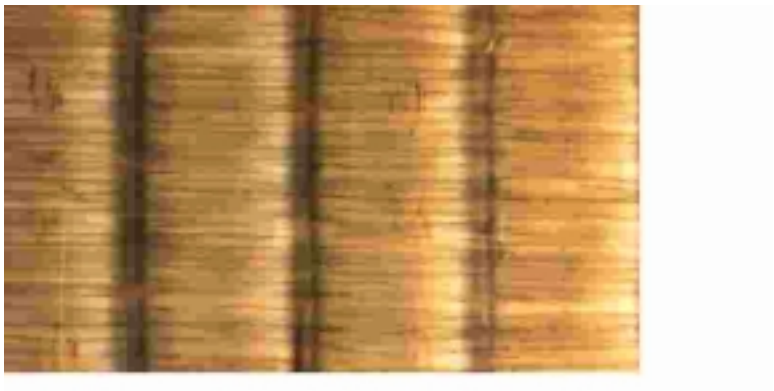

Figure 5 Transmitted light photograph showing the saturation point of the transverse cracks within NLI structure tested along the warp direction

Secondary softening*:* In most of the specimens a second change in the stiffness was observed at about 9000 με and about 250 MPa. The presumable explanation for second softening appearance at high strain is that it was caused by easier straightening of load bearing tows. For a final conclusion more tests have to be conducted.

Longitudinal cracking: Small cracks occur in the warp tows in the load direction. These longitudinal cracks span the warp tow thickness. These cracks first appeared in the outermost warp tows, and were also most numerous in these tows. Cracks appeared to initiate under the binder/warp tow crossover point then it seemed to propagate within the tow. These initial longitudinal cracks can be seen in the next photograph.

Local disbonding**:** These disbonds occurred in the region immediately surrounding the warp tow/binder crossover point at fibre resin interface. These disbonds looked like dark ellipses and are visible in Figure 6.

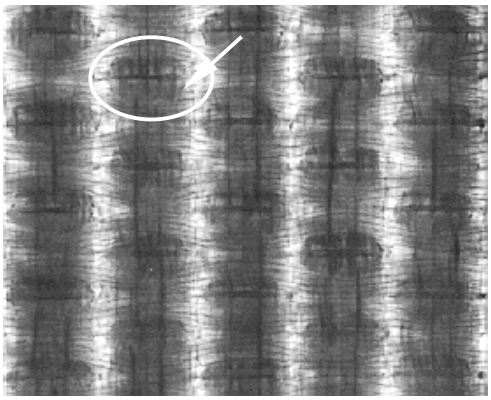

Figure 6 Transmitted light photograph showing local disbonding

Some specimens developed large local disbonds that were almost circular. These large disbonds coincided with locations of wavy weft cracks.

***Failure*:** Lengthening of longitudinal cracks, increased the number of transverse cracks and propagation of local disbonds. These features were followed by gross cracking across specimen and longitudinal tow lifting. All these failure "events" determine the specimens' eventual final failure.

The most obvious difference between the testing direction consisted in the way the sample failed. If tested along the warp the failure region was narrow whilst the samples tested along the weft failed in a very large region

When tested along the warp the binder tends to remain in place, holding the preform together. The main conclusion is that additional stresses are introduced to the binder when tested along the weft, which initiate binder rupture and produce the warp and weft release. It seems to be a "delocking" of warp and weft yarn tows.

Possible Damage progression / Damage mechanisms.

The investigation of surface photographs, taken during testing, and the micrographs of failed specimens helped to identify three types of damages. These damage features are: 1) transverse cracks, 2) longitudinal cracks (not shown) and 3) local disbonds.

The microscope investigation was considered to be the most accurate method to analyse the damage progression. The investigation of the whole sample's cross-section under the microscope proved that the surface damage was throughout the cross-section.

In [1] it is shown that the cracks follow a path which has the length of a unit cell. The appearance and direction of these cracks depends on the yarn's crimping angles or weaviness.

As was discussed in [1] and in related work shown in [7] and [8], a crimped warp is described by

$$z_w = h_w \sin(2\pi y/2\lambda_f) = h_w \sin(\pi y/\lambda_f) \quad (1)$$

and a crimped weft is described by

$$z_f = h_f \sin(\pi x/\lambda_w). \quad (2)$$

Also, in [1], it is shown that

$$\frac{dz_w}{dy} = \frac{h_w \pi}{\lambda_f} \cos\frac{\pi y}{\lambda_f} = \tan\alpha_w \quad (3)$$

These parameters are described in the schematic diagram shown in Figure 7. The subscripts 'f' and 'w' represent the weft and warp yarns respectively.

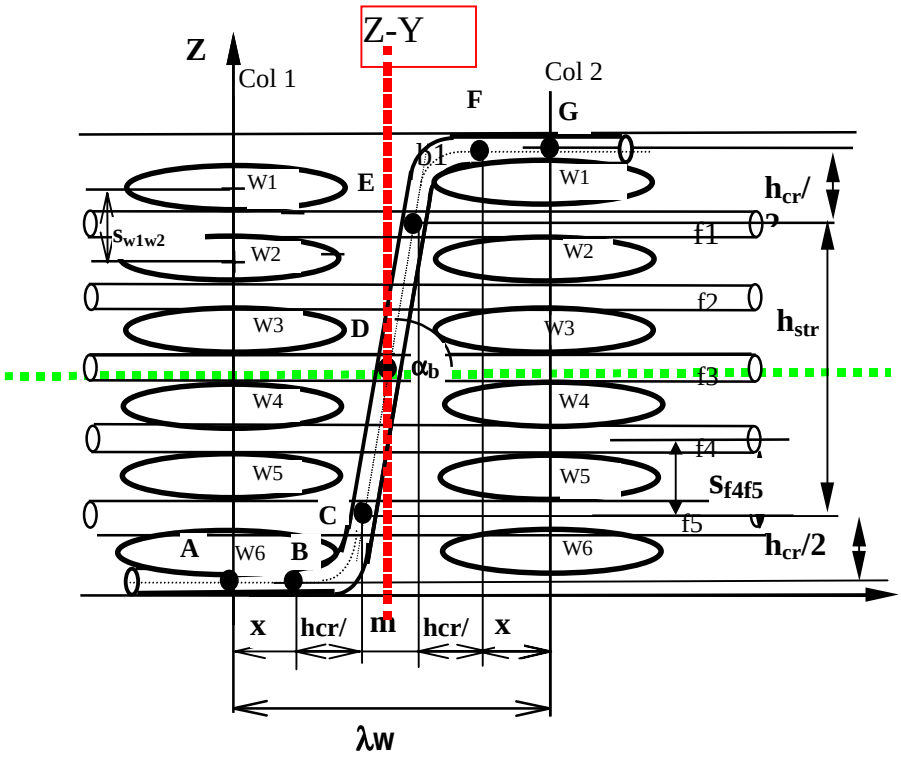

Figure 7 A Unit cell showing Geometric Parameters

Therefore, a crimped yarn is described by Equ (4)

$$\frac{dz_f}{dx} = \frac{h_f \pi}{\lambda_w} \cos\frac{\pi x}{\lambda_w} = \tan\alpha_f. \qquad (4)$$

It is obvious that the maximum value of $\tan\alpha_w$ occurs when

$$\alpha_{w\,max} = \tan^{-1}\left(\frac{h_w \pi}{\lambda_f}\right) \qquad (5)$$

$$\alpha_{f\,max} = \tan^{-1}\left(\frac{h_f \pi}{\lambda_w}\right) \qquad (6)$$

where λ_f ,λ_w represent the wavelength (pitch length) and h_w and h_f represent the amplitude. The crimping angles have a maximum value for the $\frac{h_w}{\lambda_f}$ and $\frac{h_f}{\lambda_w} = 0.4$. While the crimping angle, for warp and wefts, vary between 0 and 45^0, the ratio between crimping amplitude and wavelength vary between 0 and 0.4.

The implication of yarn undulation on transverse cracks formation is depicted in Figure 8 below.

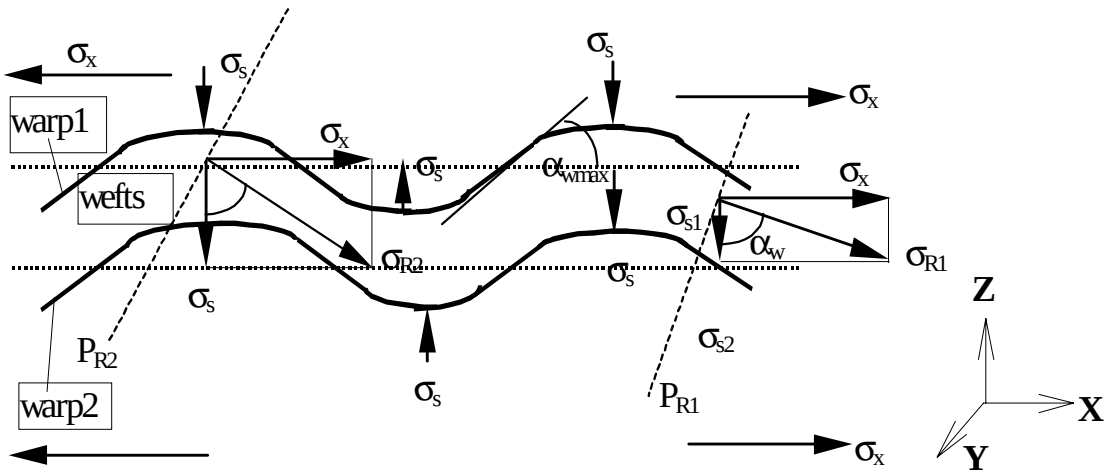

Figure 8. Implication of yarn geometry undulation on transverse cracks formation

Consider the case of two consecutive crimped warps, warp 1 and warp 2, as in figure above. Their spatial position in the XYZ coordinates is given by the Equations (1). The space between their outer boundaries is occupied by weft tows. During the tensile testing (along the warp direction) the warps are subjected to constant tensile stress $\boldsymbol{\sigma_x}$. The fact the cracks occurred under an angle other than 90 ^{o} to the X axis, or the loading direction, indicates that along with pure tensile stresses there were other stresses introduced by crimping. As was explained earlier, the crimped yarns under pure tension tended to flatten out and thus the straightening stresses $\boldsymbol{\sigma_s}$ were introduced. The resolved stress $\boldsymbol{\sigma_R}$ has an orientation and a value dependent on σ_x and the crimping angle. The crimping angle is a function of the ratio h/λ. The resulting stress direction is important because the cracks within the weft tows (transverse cracks) are formed at 90^0 to $\boldsymbol{\sigma_R}$ direction. P_{R1} and P_{R2}, as shown by the dashed lines on Figure 8. These are the directions of the transverse cracks in the two points across the composite width.

The crack formation appears to be a result of a very complicated crack formation mode. It appears that all 3 modes of formation i.e. opening (I), sliding (II), and tearing (III) might be responsible at the micro-level.

Two situations were depicted in the above picture demonstrating that the resulting stress (σ_{R1} and σ_{R2}) changed its value and direction according to the crimped angle the axial stress and straightening stress $\boldsymbol{\sigma_s}$.

In the middle of a unit cell the crack angle changes its direction, from plus(+) to minus (-), exactly as the warp threads are changing the orientation within the pattern.

CONCLUSIONS

From the evidence presented here, it appears that there is definite yarn geometry-induced damage during the loading process and some of the stages of damage have been quantified. A sequence of primary softening - transverse cracking – longitudinal cracking – local disbonding and secondary softening has been identified.

The specimens developed local disbonding between the warp tow and matrix below the binder. The two architectures had slightly differing failure characteristics, in both size and shape, occurring at different load levels. The transverse cracks reduced the stiffness of the specimens by lowering the contribution of perpendicular tows to composite stiffness. The longitudinal cracks and local disbonds had a small effect on stiffness. Three causes have been identified as being responsible for the reduction in strength: crimping of fibres as shown in Figure 2, resin rich areas and damage to the fibres during the weaving process. Different architectures have been designed to reduce fibre crimping and disperse resin rich areas in an attempt to improve mechanical properties of the material.

Further investigation of the effects of the damage features discussed in this work is required. Although the damage features found did not affect the material properties to a large extent in tension testing, this may not be the case for compression, or compression after impact. Therefore, a similar study of damage features under these loading conditions may prove to be very valuable.

REFERENCES

1. Coman F (1999), '*Design & Analysis of 3D Woven Composites'*, Ph.D Thesis, RMIT University, Melbourne, Australia.
2. Coman, F., Herszberg, I., Bannister, M., John, S., *A realistic computer simulation of multilayer woven structure,* CADCOMP 1996, Italy.
3. Ding, Y.Q., Wenger, W., McIlhagger, R., *Structural Characterisation and Mechanical Properties of 3-D Woven Composites***,** SAMPE 1993.
4. Arendts, F.J., Drechsler, K, Brandt, J., *Manufacturing and Mechanical Performance of Composites with 3-D Woven Fibre Reinforcement***,** 4th Textile Structural Composites Symposium, Philadelphia, July 1989.
5. Byun, J.H., Chou, T.W. *Elastic Properties of 3-D angle-interlock Fabric Preforms*, J.Text.Inst., 1990,81 No 4.
6. Sabu John, Floarea Coman, Israel Herszberg, Michael Bannister, "Correlation of Weave Parameter-Micromodels of 3D Woven Composite Structures with its Macromechanical Properties". Proceedings of the 4th Intl. Conference on The Deformation & Fracture of Composites, Manchester, UK, March 1997.
7. Guess, T. R., Reedy E.D.Jr., *Comparison of Interlock Fabric and Laminated Fabric Kevlar 49/Epoxy Composites*, Journal of Composites Technology & Research, Vol. 7 No 4, 1985, pp136-142

8. Coman, F., Herszberg, I., Bannister, M., John, S.,"*Computer Modelling of 3D Woven Preforms for Composite Structures"*, presented at the Sixth Australian Aeronautical Conference, Melbourne, Australia, 20 - 23 March, 1995.

9. Cox B., *Failure models for textile Composites*, NASA Contractor Report, August 1995, Rockwell International Science Center, Thousand Oaks, California, USA.